Detection of spheriodal free oscillation excited by Peru 8.2 M_s earthquake with five international superconducting gravimeter data

LEI Xiang'e, XU Houze & SUN Heping

Key Laboratory of Dynamic Geodesy, Institute of Geodesy and Geophysics. Chinese Academy of Sciences, Wuhan 430077, China
Correspondence should be addressed to Lei Xiang'e (email: leixe@asch.whigg.ac.cn)

Abstract   In this paper, authors obtain the spectral peaks of the earth free oscillation and check all normal modes from $_0S_0$ to $_0S_{48}$ accurately, with the Fourier analysis and the maximum entropy spectrum method dealing jointly with six groups of the observational residual data from five international superconducting gravimeter stations. By comparing the observational results in this paper with three former groups of observations or models, authors notice an extra discrepancy between two observational $_0S_2$ modes excited separately by Peru earthquake and Alaska earthquake, which probably mirrors the anisotropy of the Earth's inner core. The analysis on the splitting $_1S_2$ mode shows that the asymmetric factor of rotationwise spectral splitting is possible to be different from that of anti-rotationwise spectral splitting.

People have begun to research the Earth free oscillation (EFO) since the 19th century, but the mature theories of EFO came into being by the end of the 1960s[1]. EFO includes two basic categories: toroidal modes $_nT_l^m$ and spheroidal modes $_nS_l^m$, in which subscript n gives the numbers of surfaces (along a radius) of null displacement, index m is the class in longitude and index l is the degree in latitude[2]. All modes of EFO can be theoretically calculated by employing the numerical integration on the basis of elastic movement equations. When an earth model adopts a different distribution of density and Lame parameters, the computed theoretical periods of EFO will also be different. So the observational periods of EFO provide a kind of important observation data of examining the inner construction of the Earth[3].

In 1960, the phenomenon of EFO was first observed separately by Benioff group[4] with the strainmeter and Ness et al.[5] with spring gravimeter, which opened the prologue of the observation for EFO. Since then, all observation results including completely in the spheriodal normal modes of EFO are always provided by the long-period seismographs or spring gravimeters. Since the middle period of the 1980s the superconducting gravimeters (SG) were used to observe the gravity field of the Earth, Van Camp[6], Neumeyer[7] and Lei et al.[8,9] have investigated the phenomena of EFO with SG, but only part of the spheriodal modes of EFO are obtained. In this paper, authors have checked all modes from $_0S_0$ to $_0S_{48}$, by analyzing six sets of observation data from five international SG stations.

The hypothesis[12,13] on the anisotropy of the Earth's inner core was put forward because of the discoveries of the abnormal travel times of PKIKP waves[10] and the anomalous splitting of EFO[11], but later some people noticed the difference between the observational results of PKIKP waves and those of EFO. In this paper, the discussion on the anisotropy of the inner core supports the observation results of PKIKP waves, and authors find that the asymmetric factor of rotationwise spectral splitting is probably different from that of anti-rotationwise spectral splitting.

1 Introduction to five international SG stations

The main goals of the Globe Geodynamic Project (GGP) are to research all kinds of the geophysical and geodynamic phenomena by employing the continuous and synchronous observations of SGs distributed in the globe. Institute of Geodesy and Geophysics, Chinese Academy of Sciences is the only international cooperative companion of GGP in China. To study the EFO excited by Peru large earthquake (8.2Ms; June 23, 2001), authors collected the observational data of SG coming separately from Sutherland station in South Africa, Membach station in Belgium, Metsahovi station in Finland and Vienna station in Austria, besides Wuhan station in China. Because the Dual sphere SG in Sutherland station provides two sets of observations including high sphere recordings and low sphere recordings, we can apply six sets of data from five international SG stations to research into the phenomena of EFO. In table 1, authors list some information on five SG stations (for example: the positions, height, instrumental models, sampling ratio, and the calibration values of SGs and the calibration values of pressure recordings).

2 Processing of observational SG data

The analysis process of observational SG data consists of three steps: the pre-treatments of original observation data of SG, the analysis for one group of observational SG data and the spectral analysis for six sets of observational residuals.

2.1 Pre-treatments of original observation data of SG

For the convenience to analysis, six sets of observational SG data need to be translated into the same sampling period of 10 seconds. To realize this aim, the spline interpolation at the 3rd order is used for the observation data from Wuhan station, authors take one sample from every two recordings from Sutherland station and take one sample from every ten recordings from Metsahovi station or Vienna station. Occasionally, there exist some recording points from Menbach station, Metsahovi station or Vienna station returning to zero or exceeding the recoding limit of SG, so it is necessary for us to do some suitable pre-treatments for these abnormal recording points. The observation data of SG and the pressure recordings may be obtained by utilizing the calibration values to the original recordings from five international SG stations.

2.2 Analysis for one group of the observational SG data

This process includes three steps: the removal of gravity tides, the correction of pressure and the Fourier analysis for observational residuals.

The tidal parameters of these five SG stations have been accurately determined and they are the average observation results of gravity tides in several

Table 1 Some information on five international SG stations

Stations	Wuhan	Sutherland	Membach	Metsahovi	Vienna
Latitude/(°)	30.52	−32.3812	50.6093	60.2172	48.2493
Longitude/(°)	114.49	20.8109	6.0066	24.3958	16.3579
Height/m	80	1791	250	55.6	192.44
SG model	C031	D037	C021	T020	C025
Calibration of SG/μGal $\cdot$ V^{-1}	−84.655	−69.35	78.420	1.0	−77.8279
Calibration of pressure/μGal $\cdot$ V^{-1}	557.254	1.00	133.322	1.0	−133.2895
Sampling ratio/s	20	5	10	1	1

years[14]. However the phenomena of EFO only keep a few days[1], so the present scholars do not usually adopt the method of synthetic tides but employ the low-passing or zone-passing digital filters to remove the gravity tides[6,7]. In view of the unsatisfied frequency-phase characteristics of some digital filters, authors use the method of fragmental polynomial fitting to remove the gravity tides[15]. It is very important to choose the suitable class of fitting polynomials depending on the passage length of observation data to remove the gravity tides, and our experiments show that the gravity tides can be effectively eliminated from the observational SG data of 22 hours by using the fitting polynomial of the 20th class[8,9].

Sun[16] use the method of atmospheric Green function to obtain the atmospheric gravity admittance $(-0.3603 \times 10^{-8}$ m $\cdot$ s^{-2}/hPa) at Wuhan station, and Xu et al.[17] get the atmospheric admittance $(-0.307 \times 10^{-8}$m $\cdot$ s^{-2}/hPa) by taking the regression analysis for the observational SG data from Wuhan station. For the detection of EFO, authors take an average value $(-0.326 \times 10^{-8}$ m $\cdot$ s^{-2}/hPa) as the atmospheric admittance at Wuhan station to do the pressure correction. For the different observation situations around these stations, the atmospheric admittances at different SG stations are not possible to be one value, but the approximate value of them is usually equal to -0.3×10^{-8} m $\cdot$ s^{-2}/hPa. For the related detailed discussions on the pressure correction refer to some relevant papers[8,17].

Six sets of power spectra of observation residuals are obtained. By applying the discrete Fourier transform (DFT)[15] to six groups of observational residuals with the correction of gravity tides and pressure from five international SG stations. The analysis results show that the low frequency modes of EFO are clearly checked in three sets of power spectra of observation residuals from Wuhan station and Sutherland station, and the higher class modes of EFO are finely investigated in three sets of power spectra of observation residuals from three SG stations in Europe. Banka[18] introduced a method of noise magnitude of earthquake (abbrev: Mn method) to appraise the observation noise

of SG during the period of EFO, which took the power spectrum of observation residuals in the range of 1.67—9.9 mHz as the noise spectrum of SG, however there are the abundant spectral peaks of modes of EFO in this frequency range actually. In view of this reason, authors apply the power spectrum of the observational residuals of SG during the instruments' normal running before or after EFO to evaluating the observation noise of SG, which effectively expands the frequency range of EFO phenomena checked by SG.

2.3 Spectral analysis for six sets of observational residuals of SG

We have observed the spectral peaks of modes of EFO from every group spectrum of observational residuals, however it can only provide the spectral peaks of part modes of EFO with the low resolution ratio. The advantage of SG running stability has not be effectively utilized, so it is necessary to deal jointly with these observational residuals of SG. According to the characteristics of six groups of observation residuals, authors make use of two methods: the DFT for stacking observational residuals and the maximum entropy spectrum for part observational residuals.

（ⅰ）DFT for stacking observational residuals. A long series of residuals with the recording length of 2.58×10^6 s is obtained by stacking six sets of observational residuals. By applying the DFT with Hanning window[15], authors get the power spectrum of EFO with the resolution ratio of 3.704×10^{-7} Hz, which is marked as $F_1(\omega)$ and shown in fig. 1(a). $F_1(\omega)$ has checked all normal modes from $_0S_0$ to $_0S_{48}$ except $_0S_2$ mode. To investigate the more clear spectral peaks of low class modes especially $_0S_0$—$_0S_5$ modes, authors construct another long series of residuals consisting of three groups of observational residuals from Wuhan SG station and Sutherland SG station, which has a recording length of 1.29×10^6 s. By employing the Fourier analysis, authors gain another power spectrum of EFO with the resolution ratio of 7.407×10^{-7} Hz and it is marked as $F_2(\omega)$ and shown in fig. 1(b).

（ⅱ）Maximum entropy spectrum for part observational residuals. In the back of three sets of obser-
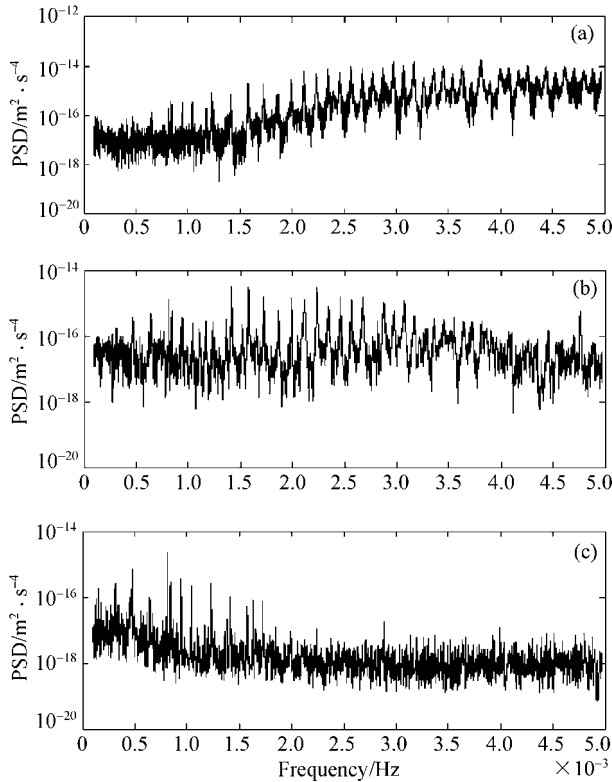
Fig. 1. The spectra peaks of EFO excited by Peru earthquake (8.2 M_s, 20016.23). Abscissa axis is the frequency (f), longitudinal axis is the power spectral density (PSD). (a) $F_1(\omega)$ spectrum; (b) $F_2(\omega)$ spectrum; (c) $S(\omega)$ spectrum.

vational residuals from Wuhan station and Sutherland station, there exist three passages of continuous stable signals of EFO, which may be looked on as three passages of stationary random signals according to the view of statistics. So we can apply the maximum entropy spectrum (Burger method)[15] to these three passages of continuous stable signals, and three groups of observational power spectra of EFO are gained and marked separately as $S_1(\omega)$, $S_2(\omega)$ and $S_3(\omega)$. The observational power spectrum of EFO are finally represented as:

$$S(\omega) = \left[\prod_{i=1}^{3} S_i(\omega) \right]^{1/3},$$

which has a resolution ratio of 1.770×10^{-6} Hz and is shown in fig. 1(c) . During the back period of EFO, the high frequency modes have been fully decayed, and only some low class modes of EFO (for example:

$_0S_0$—$_0S_5$) can be clearly checked by $S(\omega)$.

3 Determination of normal modes of EFO

Authors adopt the weighted mean values of three observational results separately from $F_1(\omega)$, $F_2(\omega)$ and $S(\omega)$ as the observed values of some low class modes (for example: $_0S_0$—$_0S_5$), and the weighted factors are the reciprocals of the frequency resolution ratio and in the proportion of 4.78 : 2.39 : 1. Because $_0S_2$ mode is not checked in $F_1(\omega)$, the observed $_0S_2$ mode is the weighted mean value of two observational results from $F_2(\omega)$ and $S(\omega)$. The normal modes of $_0S_6$—$_0S_{48}$ are excellently observed in $F_1(\omega)$, so they are directly adopted as the observational results in this paper. In table 2, authors list all normal modes from $_0S_0$ to $_0S_{48}$ checked by SG, and three groups of former observational results provided separately by Slichter et al.[1,4], Derr[19] and Dziewonski & Gilbert[20] with the conventional instruments and three sets of theoretical results separately from HB1 Model[1,21], Derr Model[19], and Jordan & Anderson Model[22].

SG possesses a wide linear dynamic range, low noise and instrument drift, which is now considered as the most reliable instrument to measure the small change of the Earth gravity field[23]. Since the 1990s, some international scholars have carried out the research on EFO with SG, however there has not been a set of complete observational results of normal modes of EFO checked by SG. In this paper, authors first provide a set of complete observational results of all normal modes from $_0S_0$ to $_0S_{48}$ checked by SG. On the one hand, Peru earthquake (8.2 M_s) was so huge to excite all normal modes, especially some low class modes: $_0S_2$ and $_0S_3$, on the other hand, authors apply the method of fragmental polynomial fitting to removing the gravity tides, which helps to deal jointly with six groups of the observational residuals, and the following spectral analysis technique can effectively improve the resolution ratio of the power spectrum of EFO. At the same time, authors do not follow the former analysis method on the observation noise of SG (the Mn method[18]), but introduce a new method of using the power spectrum of the observational residuals during the instruments' normal running before or

Table 2　The comparison between observed results in this paper and three groups of former observations or theoretical predictions on all modes from $_0S_0$ to $_0S_{48}$

Modes	Observed by this paper (s)	Ob_1 (s)	Ob_2 (s)	Ob_3 (s)	Th_1(s)	Th_2(s)	Th_3 (s)
$_0S_0$	1227.54	1227.7	1227.64	1227.64	1228.8	1227.19	1227.61
$_0S_2$	3224.97	3233.1	3233.30	3233.30	3226.9	3232.39	3232.45
$_0S_3$	21129.01	2139.2	2133.56	2133.56	2135.6	2134.08	2134.13
$_0S_4$	1546.0	1546.0	1547.16	1547.30	1547.2	1545.71	1545.82
$_0S_5$	1190.65	1188.4	1189.30	1190.12	1191.4	1190.57	1190.42
$_0S_6$	963.16	962.3	963.94	963.17	964.3	964.18	963.72
$_0S_7$	812.31	809.1	811.67	811.45	812.5	812.95	812.24
$_0S_8$	707.55	707.7	707.57	707.64	707.9	708.54	707.70
$_0S_9$	634.00	634.0	634.01	633.95	633.9	634.47	633.69
$_0S_{10}$	579.98	579.3	580.04	580.08	579.4	579.81	579.19
$_0S_{11}$	535.92	536.8	536.46	536.56	537.1	537.28	536.87
$_0S_{12}$	502.03	502.3	502.03	502.18	502.6	502.56	502.34
$_0S_{13}$	473.19	473.2	473.05	473.14	473.5	473.26	473.21
$_0S_{14}$	447.92	448.4	448.37	448.28	448.4	448.01	448.10
$_0S_{15}$	426.14	426.3	426.19	426.24	426.4	425.94	426.16
$_0S_{16}$	406.50	406.8	406.54	406.77	407.0	406.46	406.79
$_0S_{17}$	389.60	389.3	389.37	389.31	389.7	389.13	389.56
$_0S_{18}$	373.84	373.9	373.39	373.89	374.2	373.59	374.10
$_0S_{19}$	360.51	361.5	360.57	360.20	360.1	359.57	360.14
$_0S_{20}$	347.87	347.3	347.39	347.82	347.4	346.84	347.47
$_0S_{21}$	336.14	335.8	335.80	336.00	335.8	335.21	335.88
$_0S_{22}$	325.48	324.8	325.07	325.31	325.2	324.54	325.23
$_0S_{23}$	315.51	315.5	315.11	315.43	315.3	314.68	315.38
$_0S_{24}$	306.25	306.3	306.10	306.25	306.2	305.54	306.24
$_0S_{25}$	297.77	297.6	297.54	297.71	297.7	297.03	297.72
$_0S_{26}$	289.66	289.9	289.48	289.69	289.7	289.06	289.74
$_0S_{27}$	282.30	281.8	282.38	282.34	282.3	281.58	282.25
$_0S_{28}$	275.23	275.2	274.87	275.06	275.2	274.54	275.18
$_0S_{29}$	268.68	268.4	268.27	268.44	268.5	267.88	268.49
$_0S_{30}$	262.24	262.1	261.94	262.15	262.2	261.57	262.15
$_0S_{31}$	256.27	256.2	256.02	256.00	256.2	255.57	256.12
$_0S_{32}$	250.20	250.3	250.09	250.20	250.5	249.87	250.38
$_0S_{33}$	245.16	245.0	245.30	244.95	245.0	244.42	244.91
$_0S_{34}$	239.53	239.8	239.87	239.70	239.8	239.22	239.67
$_0S_{35}$	234.68	234.9	234.51	234.69	234.8	234.24	234.66
$_0S_{36}$	229.69	229.9	229.66	229.74	230.0	229.46	229.85
$_0S_{37}$	225.40	224.9	224.75	225.16	225.4	224.88	225.24
$_0S_{38}$	220.90	219.8	220.08	220.62	220.9	220.48	220.80
$_0S_{39}$	216.58	216.4	216.45	216.43	216.6	216.24	216.54
$_0S_{40}$	212.46	212.3	212.09	212.31	212.5	212.16	212.43
$_0S_{41}$	208.22	208.3	207.88	208.05	208.5	208.23	208.47
$_0S_{42}$	204.64	204.7	204.54	204.57	204.7	204.43	204.65
$_0S_{43}$	200.87	200.8	201.00	200.93	200.9	200.77	200.96
$_0S_{44}$	197.11	197.6	197.51	197.19	197.3	197.23	197.40
$_0S_{45}$	193.79	194.0	193.91	194.03	193.9	193.80	193.95
$_0S_{46}$	190.57	191.2	190.89	190.59	190.5	190.49	190.62
$_0S_{47}$	187.51	187.4	187.48	187.43	187.2	187.29	187.40
$_0S_{48}$	184.11	184.3	184.29	184.25	184.1	184.18	184.27

　　Ob_1, Ob_2 and Ob_3 were observed separately by Slichter et al., Derr and Dziewonski & Gilbert; Th_1, Th_2 and Th_3 were provided by HB$_1$ Model, Derr Model and Jordan & Anderson Model.

after EFO to appraise the observation noise of SG[8,9], which can effectively broaden the frequency range checked by SG on EFO phenomena.

For a convenient comparison between three groups of former observational or theoretical results and the observation results in this paper checked by SG, we define the relative deviation (RD) of every mode as the ratio of the discrepancy between the former published observational or theoretical value and our observational value to our observational value. In addition, we divide all modes of $_0S_0$—$_0S_{48}$ into eight mode areas called the range of normal modes (abbrev.: RNM), the average relative deviation (abbrev.: ARD) of every RNM may be obtained by calculating the average value of the relative deviations of six normal modes in this RNM. In fig. 2(a), authors plot ARD of the three groups of former observations or models in eight RNM. ARD of the observation of Slichter et al. or Derr is usually no more than 1.5‰. The observation of Dziewonski & Gilbert (abbrev.: DG Observation) is considered as one of the best observational results of

EFO, and it was obtained by analyzing the observational recordings of Alaska earthquake (8.5 M_s) provided by 84 seismic stations in the globe and employing the spectral analysis technique of high resolution ratio. ARD of DG observation is usually no more than 0.5‰ and the high limit is less than 1.0‰. ARD of HB1 model, Derr model or Jordan & Anderson model (abbrev.: JA Model) is generally no more than 1.0‰. JA Model was obtained by the joint inversion of three types of seismological information: body-wave travel times, surface wave dispersion and free oscillation periods, which adopted an earth model similar to HB1 model and accepted the conception of the solid inner core of Derr model, it is one of the fairly fine spherical symmetrical earth models of studying the EFO. ARD of JA Model is usually not more than 0.75‰, and the maximum is less than 1.0‰. In fig. 2(b), we plot the relative deviations (RD) of all modes from $_0S_0$ to $_0S_{48}$ between DG Observation or JA Model and our observational results in this paper. The relative deviations (RD) of all modes are usually not more than 1.0‰ and
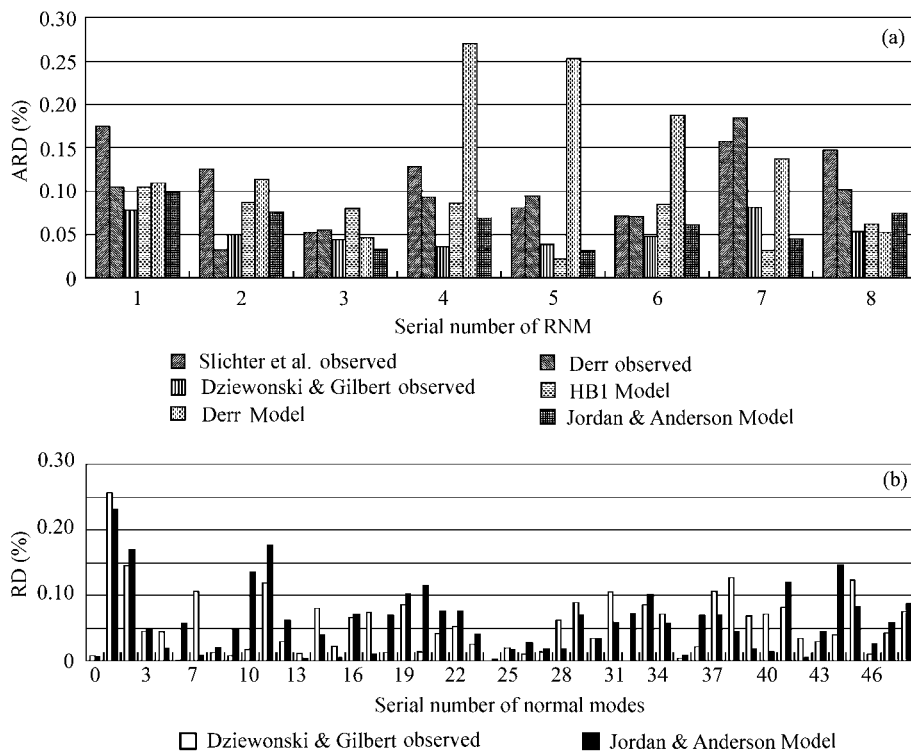
Fig. 2. Comparison between three former observations or theoretical predictions and the observational results in this paper. (a) Average relative deviation (ARD) of three former observations or theoretical predictions in eight RNM; (b) relative deviation (RD) of DG observation or JA Model from $_0S_0$ mode to $_0S_{48}$ mode.

RD of few modes exceed 1.5‰. Authors are surprised to see an extra spectral peak of about 540 s near $_0S_{11}$ mode in $F_1(\omega)$, but there is no mode of EFO in JA Model according to the extra spectral peak. This maybe helps to explain why the relative deviation of $_0S_{11}$ mode in JA Model arrives at 1.8‰, however it is not possible to be explained by the similar reason that the relative deviations of $_0S_2$ mode and $_0S_3$ mode in DG Observation separately arrive at 2.6‰ and 1.4‰. Because the relative deviations of nearly all modes in JA Model are generally no more than 1.0‰, we think that there are the extra relative deviations of about 1.6‰ and 0.4‰ for $_0S_2$ and $_0S_3$ mode between DG Observation and the observational results in this paper. The observation data of EFO was mainly coming from DG Observation during the inversion of JA Model, so the $_0S_2$ and $_0S_3$ mode of JA Model also occupy some extra relative deviations.

4 Anisotropy of inner core and investigation of anomalous spectral splitting of EFO

Poupinet et al.[10] found the abnormal travel times of PKIKP waves by analyzing the observational data of PKIKP body waves passing through the Earth's inner core, and Masters & Gilbert[11] noticed the anomalous spectral splitting of EFO. To explain the abnormal travel times of PKIKP waves and the anomalous spectral splitting of EFO, Morelli et al.[12] and Woodhouse et al.[13] put forward the hypothesis on the anisotropy of the inner core. They suggested that the Earth's inner core was axisymmetric anisotropy and the symmetric axis of the inner core was basically according to the rotation axis of the Earth. Birth[24] measured the density and sound speed of different elements by doing the experiments of impact waves, and his research manifests that the iron is the only one of main elements whose density under the pressure of the inner core is in agreement with the density of the inner core. Some investigations on mineralogy (given by Anderson[25] and Stixrude & Cohen[26]) show that the hexagonal close packed (hcp) iron (ε-phase) is the most likely phase on the conditions of the inner core, and the directional distributions of ε-phase iron will cause the anisotropy of the inner core. Both Creager[27] and Shearer[28] also discover that P wave propagation

in the north-south direction is faster than that in the equatorial direction by 3% in the inner core. But there still exist some differences between the observational results of P waves and that of EFO, Shearer[29] and Song & Helmberger[30] consider that there is an approximately isotropy zone within a range of about 150 km in the top of the inner core by analyzing the travel times of body waves, Durek & Romanowicz[31] point out that the top part of the inner core should be large anisotropy to explain the known anomalous spectral splitting of EFO.

The rotation and ellipticity of the Earth can cause the spectral splitting phenomena of EFO, which are often looked on as the normal spectral splitting of EFO, the spectral splitting phenomena that can not be explained by the rotation and ellipticity are usually considered as the anomalous spectral splitting of EFO. Backus & Gilbert[32], MacDonald & Ness[33] and Pekeris et al.[34] separately applied the perturbation theories to studying the spectral splitting and shift caused by the rotation of the Earth. Caputo[35] analyzed the effect of the Earth's ellipticity on the spectral shift of EFO. Dahlen[36,37] comprehensively summarized the influences of the Earth's rotation and ellipticity on the spectral splitting of EFO, which can be represented as the following expression:

$$_n\omega_l^m / {}_n\omega_l = 1 + {}_n a_l + m({}_n\beta_l) + m^2({}_n\gamma_l)$$
$$(m = -l, \cdots, 0, \cdots, l).$$

In this expression, $_n\omega_l$ is the theoretical frequency of one mode of a SNREI Model, $_n\omega_l^m$ is the splitting and shift frequency caused by the Earth's rotation and ellipticity. The splitting parameters of EFO include $_n\alpha_l$, $_n\beta_l$ and $_n\gamma_l$. Among them, $_n\alpha_l$ is the floating parameter of central frequency (abbrev.: FPCF), $_n\beta_l$ is the spectral splitting parameter of the rotation (abbrev.: SSPR), $_n\gamma_l$ is the asymmetric factor of spectral splitting (abbrev.: AFSS) and it is mainly influenced by the Earth's ellipticity. Woodhouse et al.[12] introduced a method of spectral splitting function to investigate the construction of the Earth's inner core with the observational data of EFO, the function of

spectral splitting can be represented as

$$f(\theta,\phi) = \sum_{s,t} C_s^t Y_s^t(\theta,\phi).$$

In this expression, $s = 0, 2, \cdots, 2l$; $t = -s, -s + 1, \cdots,$ s; C_s^t is the factor of the spectral splitting function (the function related to radius), $Y_s^t(\theta,\phi)$ is the spherical harmonic function, θ and ϕ are latitude and longitude. When some scholars[31] applied the method of spectral splitting function to studying the phenomena of EFO, $_{13}S_2$ was one of the most usually adopted modes in this method. On the influence of the characteristics of the integration kernel function $K^S(r)$ of C_s^t, the spectral splitting function $f(\theta,\phi)$ is sensitive to the physical parameters in the top of the inner core, but insensitive to the situations in the deep of the inner core. This is possible to be a fairly important reason to explain the difference between the analysis results of PKIKP waves and those of EFO on the structure of the inner core. A noticeable fact is that the observational spectral peaks of $_{13}S_2$ mode appear very low and dim usually, so there are some actual difficulties in determining the $_{13}S_2$ mode of EFO accurately.

$_0S_2$ mode and $_1S_2$ mode have been clearly observed in $F_2(\omega)$. The observational $_0S_2$ mode includes two spectral splitting peaks $_0S_2^{-2}$ (3.01052×10^{-4} Hz) and $_0S_2^1$ (3.14737×10^{-4} Hz) shown in fig. 3(a), and the observational $_1S_2$ mode consists of three spectral

splitting peaks $_1S_2^{-2}$ (6.740741×10^{-4} Hz), $_1S_2^0$ (6.807407×10^{-4} Hz) and $_1S_2^2$ (6.859259×10^{-4} Hz) shown in fig. 3(b). Dahlen[36] has given the theoretical splitting parameters of some modes from three SNREI Models, and the theoretical splitting parameters of $_0S_2$ and $_1S_2$ mode (the average values) are written on the following lines:

$$_0\alpha_2 = 0.984‰, \quad _0\beta_2 = 14.916‰, \quad _0\gamma_2 = -0.545‰;$$

$$_1\alpha_2 = 1.212‰, \quad _1\beta_2 = 4.078‰, \quad _1\gamma_2 = -0.438‰.$$

If the theoretical frequencies of $_0S_2$ mode (3.09282×10^{-4} Hz) and $_1S_2$ mode (6.79879×10^{-4} Hz) in JA Model are looked on as the theoretical central frequencies of the two modes and signed as $_0S_2^0$ and $_1S_2^0$, we can calculate the observed splitting parameters of $_0S_2$ and $_1S_2$ mode.

From two spectral peaks of $_0S_2$ mode observed in $F_2(\omega)$, we can deduce the observational value of SSPR $_0\beta_2^* = 14.724‰$ in good accordance with the theoretical value of SSPR $_0\beta_2$. Though three splitting peaks of $_0S_2$ mode have been checked in $S(\omega)$, we have not yet gained the effective observational value of AFSS of $_0S_2$ ($_0\gamma_2^* \leqslant 0.01‰$) like the former scholars. In table 2, the observational value of $_0S_2$ mode (3.10080×10^{-4} Hz according to 1/3224.97s) is a weighed average value of two central frequencies of $_0S_2$ observed in $S(\omega)$ and $F_2(\omega)$, which may be looked on as the observational value of central frequency of $_0S_2$ mode and
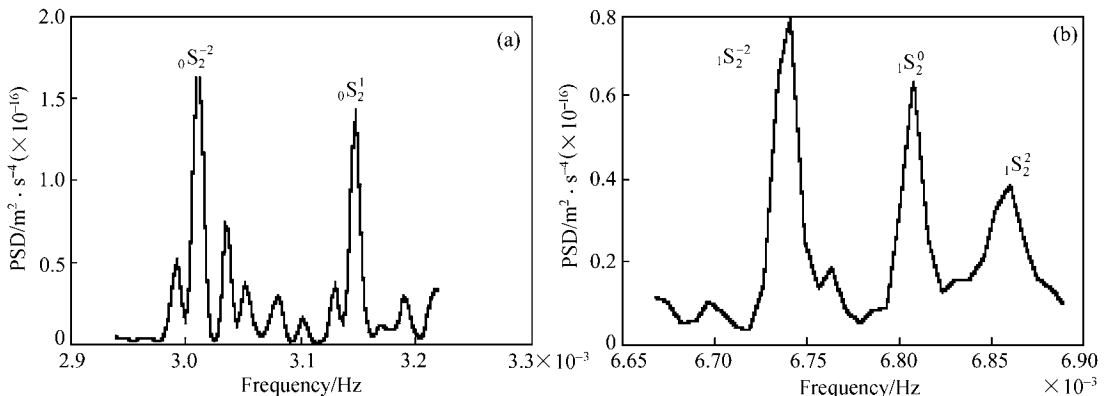
Fig. 3.   The splitting $_0S_2$ mode and $_1S_2$ mode in $F_2(\omega)$ spectrum. Abscissa axis is the frequency (f), longitudinal axis is the power spectral density (PSD). (a) $_0S_2$ mode; (b) $_1S_2$ mode.

signed as $_0S_2^0*$. There exists a relative deviation of $_0\alpha_2^*$=2.56‰ between the observed central frequency $_0S_2^0*$ and the theoretical central frequency $_0S_2^0$ given by JA Model, which is more than 2.40‰ the relative resolution ratio of $F_2(\omega)$ near $_0S_2$ mode and cannot be explained by the rotation and ellipticity of the Earth yet. When Fang[1] calculated the theoretical periods of $_0S_n$ modes of EFO by the numerical integration from the Earth's surface to the center of the Earth, he found that the penetration depth of $_0S_2$ and $_0S_3$ mode entered into the inner core, Among them, the penetration depth of $_0S_2$ mode reached near the center of the Earth and that of $_0S_3$ mode got into the inner core slightly. In the former paragraph, authors have pointed out that there is an extra relative deviation of about 1.5‰ between the two $_0S_2$ mode excited by Peru earthquake (16°S, 73°W) and Alaska earthquake (60°N, 150°W), which is approximately equal to the value of $_0\alpha_2^* - _0\alpha_2$. There is the smaller included angle between the rotation axis of the Earth and the nodal plane of $_0S_2$ mode excited by Peru earthquake, so it possibly propagates faster and the observed period of it is shortened about 8 s for the anisotropy of the inner core. The fact is pointed out in the former paragraph that the extra relative deviation of $_0S_2$ mode is clearly larger than that of $_0S_3$ mode, it probably implies that there exists the phenomenon of strong anisotropy in the deep of the inner core. On the base of the former analysis, authors support the observational conclusion from PKIKP waves.

We can directly calculate the observational splitting parameters: $_1\alpha_2^*$=1.265‰, $_1\beta_2^*$=4.358‰ and $_1\gamma_2^*$ = −0.272‰ from three splitting peaks of $_1S_2$ mode. The observed FPCF $_1\alpha_2^*$ is according to the theoretical FPCF $_1\alpha_2$ very well, and the observed SSPR $_1\beta_2^*$ is a little larger than the theoretical SSPR $_1\beta_2$, but the observed AFSS $_1\gamma_2^*$ is nearly equal to a half of the theoretical AFSS $_1\gamma_2$. The theoretical FPCF

and SSPR ($_1\alpha_2$ and $_1\beta_2$) inferred from the perturbation theories are in good accordance with their observational values ($_1\alpha_2^*$ and $_1\beta_2^*$), so we believe that the perturbation theories should be enough accurate to deal with the spectral splitting phenomena of EFO and is not possible to produce so large discrepancy on the computation of the theoretical AFSS $_1\gamma_2$. The theoretical value of AFSS $_1\gamma_2$ includes two parts, one is the contribution of the Earth's ellipticity (−0.338‰), and the other is the contribution of the rotation of the Earth (−0.100‰). It is obvious that the observed AFSS $_1\gamma_2^*$ is too small to explain the influence of the ellipticity.

If we investigate the spectral splitting phenomenon of $_1S_2$ mode in a new idea, we can notice that the observational value of left side relative splitting width (abbrev.: LRSW) is equal to $(_1S_2^0 - _1S_2^{-2})/_1S_2^0 = $ 9.806‰, which is in good agreement with the theoretical value of LRSW 9.908‰ deduced from the theoretical splitting parameters given by Dahlen[36]. This shows that the observed anti-rotationwise SSPR and AFSS ($_1\gamma_2^*$ and $_1\beta_2^*$) should be basically equal to the theoretical SSPR and AFSS ($_1\gamma_2$ and $_1\beta_2$). On the other hand, the observational value of right side relative splitting width (abbrev.: RRSW) is $(_1S_2^2 - _1S_2^0)/_1S_2^0 = $ 7.627‰, which is clearly larger than the theoretical value of RRSW 6.404‰ and the difference between these two values has exceed 1.09‰ the relative resolution ratio of $F_2(\omega)$ near $_1S_2$ mode. If the rotationwise SSPR $_1\beta_2^{*\prime}$ is equal to the anti-rotationwise SSPR $_1\beta_2^*$, and it also is a reasonable hypothesis for the two parameters only related with the rotation of the Earth, we can infer that the observed rotationwise AFSS is equal to $_1\gamma_2^{*\prime}$=−0.132‰, which is even less than one third of the observed anti-rotationwise AFSS $_1\gamma_2^*$=−0.438‰. The former discussions on the $_1S_2$ mode show that the rotationwise AFSS $_1\gamma_2^{*\prime}$ is clearly

1) Fang, M., Earth free oscillation—the research of some problems on the theories of resolution and inversion, Thesis for Doctor Degree, Institute of Geodesy and Geophysics, Chinese Academy of Sciences, 1991, 223.

different from the anti-rotationwise AFSS $_1\gamma_2^{*'}$, but authors do not know what Earth's dynamic effect can change the rotationwise AFSS of $_1S_2$ mode, this needs to be researched deeply in the future.

5 Conclusions and discussions

In this paper, we study six groups of observational data of Peru earthquake (8.2 M_s) recorded by five international SG stations and accurately check all normal modes from $_0S_0$ to $_0S_{48}$ by employing the Fourier analysis and the maximum entropy spectrum method for observational SG residuals.

By comparing three former observations and models with the observational results in this paper, authors find that there exists an extra relative deviation of about 1.5‰ for the $_0S_2$ modes excited separately by Peru earthquake and Alaska earthquake. On the basis of the deeper discussions on the splitting phenomena of $_0S_2$ mode, authors consider that the extra relative deviation is possible to mirror the anisotropy of the Earth's inner core.

Authors first observed the asymmetric factor of spectral splitting (AFSS) of EFO, by investigating the spectral splitting of $_1S_2$ mode. The deeper analysis demonstrates that the observational rotationwise AFSS $_1\gamma_2^{*'}$ is different from the observational anti-rotationwise AFSS $_1\gamma_2^{*}$, but this new geophysical phenomenon still needs to be confirmed in the future.

References

1. Fu, C.Y., Chen, Y.T., Qi, G.Z., Foundation of Geophysics, 2nd ed. (in Chinese), Beijing: Science Press, 1985, 347—368.

2. Garland, G. D., Introduce to Geophysics (Mantle, Core and Crust), 2nd ed., Toronto: W. B. Saunders Company, 1979, 123—133.

3. Fang, J., The free oscillation of the earth (continuation), Acta Geodaetica et Geophysica (in Chinese), 1986, 8: 53—69.

4. Benioff, H., Press, F., Smith, S., Excitation of the free oscillations of the earth by earthquake, J. Geophys. Res., 1961, 66(2): 605—619.

5. Ness, N. R., Harrison, C. T., Slichter, L. B., Observation of the free oscillation of the earth, J. Geophys. Res., 1961, 66(2): 621—629.

6. Van Camp, M., Measuring Seismic normal modes with the GWR C021 Superconducting gravimeter, Phys. Earth and Plan Int., 1999, (116): 81—92.

7. Neumeyer, J., Bathelmes, F., Combrinck, L. et al., Analysis results from the SG registration with the dual sphere superconducting gravimeter at SAGOS (South Africa), Bull D'infor Marees Terrestres, 2002, 135: 10607—10616.

8. Lei, X. E., Xu, H. Z., Sun, H. P., Check of free oscillation signal with SG data, Chinese Science Bulletin, 2002, 47(8): 1573—1578.

9. Lei, X. E., Xu, H. Z., Sun, H.P., Preliminary results of the Earth's free oscillations after Peru earthquake observed using a SG in China, Bull D'infor Marees Terrestres, 2002, 135: 10713—10715.

10. Poupinet, G., Pillet, R., Souriau, A., Possible heterogeneity of the Earth's core deduced from PKIKP travel times, Nature, 1983, 305: 204—206.[DOI]

11. Masters, G., & Gilbert, F., Structure of the inner core inferred from observations of its spheroidal shear modes, Geophys. Res. Lett., 1981, 8: 569—571.

12. Morrelli, A., Dziewonski, A.M., Woodhouse, J.H., Anisotropy of inner core inferred from PKIKP travel times, Geophys. Res. Lett., 1986, 13: 1545—1548.

13. Woodhouse, J. H., Giardini, D., Li, X. D., Evidence for inner core anisotropy from free oscillations, Geophys. Res. Lett., 1986, 13: 1549—1552.

14. Xu, H. Z., Sun, H. P., Xu, J. Q. et al., International tidal gravity reference values at Wuhan station, Science in China, Ser. D, 2000, 43(1): 77—83.

15. Ding, Y. R., Processing Method of Astronomical Data (in Chinese), Nanjing: Nanjing University Press, 1998, 190—202.

16. Sun, H. P., Atmospheric pressure and gravity, Chinese Science Bulletin, 1997, 42(1): 1712—1719.

17. Xu, J. Q., Hao, X. H., Sun, H. P., Influence of atmospheric pressure on tidal gravity at Wuhan station, Acta Geophysica Sinica (in Chinese), 1999, 28(1): 21—27.

18. Banka, D., Jentzsch, G., Crossley, D., Investigations of superconducting gravimeter records in the frequency range of the free oscillations of the Earth—the noise magnitude, Proc. 13th Symp. Earth Tides, Brussels, 1998, 641—648.

19. Derr, J. S., Internal structure of the earth inferred from free oscillations, J. Geophys. Res., 1969, 74(22): 5202—5220.

20. Dziewonski, A., Gilbert, F., Observations of normal modes from 84 recordings of the Alaskan earthquake of 1964 March 28, Geophys. J. R. astr., 1972, 27: 293—446.

21. Haddon, R. A., Bullen, K. E., An earth model incorporating free earth oscillation data, Phys. Earth and Plan. Int., 1969(2): 35—46.

22. Jordan, T. H., Anderson, D. L., Earth structure from free oscillations and travel times, Geophys. J. R. Astr., 1974, 36: 411—459.

23. Crossley, D. J., Hinderer, J., Global Geodynamics Project-GGP: status report 1994, Proceeding of the workshop on Non-tidal Gravity changes (ed. Poitevin, C.), Luxembourg: via Conseil de L'Europe Cahiers du Centre Européen de Géodynamique et de Séismologie, 1995, (11): 244—269.

24. Birch, F., Density and composition of mantle and core, J.Geophys.Res., 1964, (69): 4377—4388.

25. Anderson, O. L., Mineral physics of iron and of the core, Rev. Geophys., 1995(suppl.): 429—441.

26. Stixrude, L., Cohen, R. E., High-pressure elasticity of iron and anisotropy of Earth's inner core, Science, 1995, (267): 1972—1975.

27. Creager, K. C., Anisotropy of the inner core from differential travel times of the phases PKP and PKIKP, Nature, 1992, (356): 309—314.

28. Shearer, P. M., Constraints on inner core anisotropy from PKP (DF) travel-times, J. Geophys. Res., 1994, (99): 19647—19657.

29. Shearer, P. M., Masters, G., The density and shear velocity contrast at the inner core boundary, Geophys. J. Int., 1990, (102): 491

30. Song, X. D, Helmberger, D. V., Depth dependence of anisotropy of Earth's inner core, J. Geophys. Res., 1995, (100): 9805—9816.

31. Durek, J. J., Romanowicz, B., Inner core anisotropy inferred by direct inversion of normal mode spectra, Geophys. J. Int., 1999(139): 599—622.

32. Backus, G. E., Gilbert, J. F., The rotational splitting of the free oscillations of the earth, Proc. Natn. Acad. Sci., 1961(47): 362—371.

33. MacDonald, G., Ness, N., A study of the free oscillations of the Earth, J. Geophys. Res., 1961, (66): 1865—1911.

34. Pekeris, C. L., Alterman, Z., Jarosch, H., Rotational multiplets in the spectrum of the Earth, Phys. Rev., 1961, (122): 1692—1700.

35. Caputo, M., Free modes of layered oblate planets, J. Geophys. Res., 1963, (68): 497—503.

36. Dahlen, F. A., The normal modes of a rotating, elliptical earth, Geophys. J. R. Astr., 1968, (16): 329—367.

37. Dahlen, F. A., The normal modes of a rotating, elliptical earth-II near-resonance multiplet coupling, Geophys. J. R. Astr., 1969, (18): 397—436.

—498.